Title
PRODUCTION OF FREE RADICALS IN SOLID BIOLOGICAL SUBSTANCES BY HEAVY IONS

Author
Henriksen, Thormod.

Publication Date
1965-07-20

UCRL-16280

University of California

Ernest O. Lawrence Radiation Laboratory

PRODUCTION OF FREE RADICALS
IN SOLID BIOLOGICAL SUBSTANCES
BY HEAVY IONS

Berkeley, California

DISCLAIMER

Submitted for publication to
Radiation Research

UCRL-16280

UNIVERSITY OF CALIFORNIA

Lawrence Radiation Laboratory
Berkeley, California

AEC Contract No. W-7405-eng-48

PRODUCTION OF FREE RADICALS IN SOLID BIOLOGICAL SUBSTANCES BY HEAVY IONS

Thormod Henriksen

July 20, 1965

PRODUCTION OF FREE RADICALS IN SOLID BIOLOGICAL SUBSTANCES BY HEAVY IONS

Thormod Henriksen

Donner Laboratory and Donner Pavilion
Lawrence Radiation Laboratory, University of California
Berkeley, California
and
Norsk Hydro's Institute for Cancer Research
Montebello, Norway

July 20, 1965

SUMMARY

Several biochemicals, including amino acids, peptides, proteins, and nucleic acid components, have been exposed to a large variety of radiations and the production of secondary radicals has been studied.

The substances were irradiated at room temperature with 6.5-MeV electrons and fast stripped helium, lithium, boron, carbon, oxygen, fluorine, neon, silicon, and argon ions from the Berkeley heavy-ion linear accelerator. From the recorded ESR spectra it appears that the types of secondary radicals were independent of the stopping power of the radiation. On the other hand, the relative yields of the primary ESR centers seem to be influenced by the type of radiation.

The yield of secondary radicals was independent of the stopping power up to about 200 MeV g^{-1} cm^2. Above this value the yield decreased with increasing stopping power. The total variation within the LET range studied (up to 1.6×10^4 MeV g^{-1} cm^2) was by a factor of 2 to 5 for the different substances. The yield-versus-stopping power curves exhibit the same form as that found for the inactivation of solid enzymes and T1 bacteriophage. This observation supports the idea that

INTRODUCTION

It is well known from low-temperature experiments that the radicals observed at room temperature in irradiated solid biological substances are the result of a sequence of events started by the initial absorption of radiation energy (1 - 4). It is therefore reasonable to expect that the types and yields of these "secondary radicals" will be influenced by the local distribution of the energy absorption as well as by the temperature at which the secondary reactions proceed.

In almost all ESR work so far presented, radiations with low stopping power, such as x rays, Co^{60} γ rays, and electrons, have been used. Recently Müller et al. (5) used Po^{210} α particles, and found that the yield of radicals in several solid amino acids compared with the yield for x rays, decreased by a factor 2 to 10. Similarly, Stratten and Koehler (6) found that the radical yield in irradiated enzymes decreased by a factor 1.25 from Co^{60} γ rays to 120-MeV protons. These results indicate that the yield of secondary radicals decreases with increasing stopping power. This may be of importance if we assume that the secondary radicals are intermediates in the processes leading to biological damage.

The efficiency of different types of radiation in producing biological damage has been studied for several different systems covering a large range in LET (7 - 11). In simple systems like enzymes, for which the loss of enzymatic activity was the measured parameter, Brustad (9, 12) found that the yield was almost independent of the stopping power up to about 200 MeV g^{-1} cm^2. Above this value the yield decreases with increasing stopping power. In other systems, such as spores and cells,

which seem to require more than one absorption event in the actual target, more complicated dependence of yield upon stopping power has been reported (9).

This paper studies the production of secondary radicals in some biologically important molecules irradiated with fast heavy ions. The compounds include simple amino acids, peptides, enzymes, and nucleic acid components. These studies have a twofold purpose. In the first place, we want to extend the earlier studies on the formation of radicals in solid biological compounds to radiation covering a much broader range of stopping power than previously used. Secondly, it is hoped that these experiments, in which the production of radicals is correlated with the loss of enzymatic activity, may shed some light on the mechanisms for radiation damage.

EXPERIMENTAL PROCEDURE

The Spectrometer

The spectrometer used is of the Varian type (4500 series) with variable-temperature cavity, 100-kc/sec modulation frequency, and 9-in. magnet. The ESR signal can be fed directly into an integrator, and it is possible to record both the derivative and the integrated spectra.

The number of ESR centers in the sample was obtained from the integrated spectra by comparison with reference samples measured under the same conditions. As reference substance ordinary anthracite carbon powder, calibrated against DPPH, was used.

Sample Preparation

Glycine, alanine, reduced glutathione, and trypsin were obtained from Nutritional Biochemical Corp., and cytidine, cytosine, and

guanosine were from California Corp. for Biochemical Research. The samples were irradiated in thin layers (20 to 50 mg/cm^2) in aluminum holders covered with a thin aluminum foil (1 mg/cm^2), in the presence of air, at room temperature. Immediately after the exposure the samples were brought to liquid nitrogen temperature, transferred to glass sample tubes, evacuated, and stored at liquid nitrogen temperature until they were measured at room temperature.

The Radiation Sources

The samples were irradiated with 6.5-MeV electrons from an electron accelerator and heavy ions from the Berkeley heavy-ion linear accelerator (Hilac). With the Hilac, ions up to atomic number 18 can be accelerated to an energy of 10.4 MeV per nucleon. In these studies beams of helium, lithium, boron, carbon, oxygen, flourine, neon, silicon, and argon ions were used. Before hitting the sample, the particles penetrate some thin aluminum foils which serve to strip the ions and scatter the beam in order to get a homogeneous radiation field.

Dosimetry

The electron dose was measured by the coloring of Co glass. This system was calibrated against a Fricke dosimeter. The total dose was kept in the range 1 to 2×10^6 rad.

The dosimetry of the heavy ions was performed as previously described by Brustad et al. (13), by measuring the total charge collected by an external Faraday cup. The dose (D) given in rads is then obtained from the formula

$$D = 1.602\,(D_0/eZA)(dE/dx)\,10^{-8},$$

where D_0 is the dose or the charge collected, measured in coulombs,

eZ is the charge of the bombarding particle, A is the beam area in cm^2, and (dE/dx) is the total stopping power of the radiation, given in MeV g^{-1} cm^2.

In most of the heavy-ion work previously reported the thickness of the samples has been less than about 5 mg/cm^2. Consequently, the spread in the stopping power throughout the sample has been relatively small. In contrast, the experiments reported here have been carried out with a sample thickness of about 20 to 50 mg/cm^2. The reason for this was to obtain an ESR sample in which the number of spins could be easily measured. Consequently beams of the heaviest ions were stopped completely within the sample, and the spread in stopping power was very large. The average stopping power, which was used to evaluate the radiation dose as well as in the results presented below, has been derived in the following way:

A. When the ions were stopped completely within the sample the average stopping power was taken to be $\langle dE/dx \rangle = E/R$, where E is the total energy of the particles when they enter the sample and R is the range of the particles in the sample. The range of heavily charged particles in organic materials is not known. However, it can be calculated, to a first approximation, by using the data given by Barkas and Berger (14). (A mean excitation potential of I = 63 eV has been used for the organic compounds studied in this work).

B. When the particles penetrate the whole sample the average stopping power may be calculated from

$$\langle dE/dx \rangle = \frac{1}{t} \int_0^t f(dE/dx)dx,$$

where t is the thickness of the sample in g/cm^2, and f(dE/dx) is the

variation in the stopping power along the track of the bombarding particle, i.e., the Bragg curve. The values used in these calculations were taken from Brustad (9).

In these experiments the total dose was in the range 1 to 2×10^6 rad, and the results presented below refer to the dose 1.5×10^6 rad. The dose rate was in all experiments of the order of 1×10^6 rad/min.

The results were expressed in number of ESR centers per gram. This is a straightforward procedure for those samples in which the ions penetrate the whole sample. However, when the particles are stopped completely within the sample only the irradiated layer can be taken into consideration, and the number of ESR centers produced per irradiated gram was calculated from

$$N = N_0 \frac{w_1}{w_2} \frac{1}{R} ,$$

where N_0 is the observed number of ESR centers in the sample, w_1 is the weight of the irradiated sample, w_2 is the weight of the measured sample (i.e., w_2/w_1 is the fraction of the irradiated sample that was measured), and R is again the range of the bombarding particle given in g/cm^2.

RESULTS

Types of Radicals

Owing to experimental difficulties we have so far not been able to study the initial ESR centers. Thus, when the samples were measured for the first time they had been at room temperature for 20 minutes, and the secondary reactions had therefore taken place to a greater or lesser extent. The present study on polycrystalline samples seems to indicate that the types of secondary radicals are independent of the stopping power of the radiation.

The most pronounced changes observed for a compound irradiated with different types of heavy ions are those for reduced glutathione (GSH), which are presented in Fig. 1. It is clearly seen that in the middle of the spectrum a resonance appears that becomes more pronounced at high LET. As previously pointed out (15), there are reasons to believe that several different types of ESR centers are initially formed in this compound. Slow secondary reactions subsequently lead to the formation of sulfur radicals, and when the samples have been at 295° K for a few hours the sulfur radicals completely dominate the spectrum. The results in Fig. 1, which represents an intermediate step in these reactions, seem therefore to indicate that the relative yields of the primary species depend upon the stopping power. When the different GSH samples were kept at room temperature the spectra become gradually equal to each other, and similar to the cysteine sulfur pattern (15).

Slow secondary reactions also take place in irradiated proteins (4). Thus, the formation of sulfur radicals is a relatively slow process even at room temperature. Small qualitative changes with changing stopping power were also observed for trypsin. When this compound was measured the first time after exposure it was found that the fraction of the resonance due to sulfur radicals decreased with increasing stopping power. The variation was small, however, and the qualitative differences disappeared with time.

Quantitative Results

In Fig. 2 are presented the radical yields as a function of the stopping power for several compounds. It appears that the shape of the curves for radical yield versus stopping power is the same for both aliphatic and aromatic compounds. Small changes, if any, in the

yields are observed in going from sparsely ionizing radiation up to 40-MeV helium ions with a stopping power of about 190 MeV g^{-1} cm^2. Above this value a continuous decrease in the radical yield with increasing stopping power was found.

The results for glycine in Fig. 3 show that the yield as a function of the stopping power also depends upon the irradiation temperature. Thus, the variation in yield becomes smaller with decreasing temperature. This seems to be a general observation, and similar results were observed for the enzymes trypsin and lysozyme (16). It is of interest to note that Brustad has reported a similar effect of the irradiation temperature on the loss of enzymatic activity of trypsin (12).

It follows from the curves presented in Figs. 2, 3, and 4 that the production of secondary radicals in organic compounds exhibits the same variation with the stopping power as that previously reported for the biological damage in simple systems. Thus, similar curves have been reported for the loss of enzymatic activity as well as for the loss of infectivity of T1 bacterophage (9, 17). In Fig. 4 the results of this work for the production of secondary radicals in solid trypsin have been correlated with Brustad's data for the inactivation of the same enzyme. The correlation suggests the possibility that the secondary radicals somehow are involved in the sequence of reactions leading to the loss of the enzyme activity. The secondary radicals produced in trypsin are mainly of the two types commonly found for proteins, namely sulfur radicals in which the unpaired electrons are associated with the cysteine sulfur atoms, and radicals in which the unpaired electrons are localized in the protein backbone, probably at glycine residues (18). As mentioned above, very small qualitative changes in the trypsin spectrum with the

changing stopping power were found. This implies that for either of the two types of radicals the same good correlation exists between the number of radicals and the inactivation.

A parameter indicating the variation in the radiosensitivity can be obtained by taking the ratio of the yields for the flat portion of the curves presented above to those observed for argon ions (with stopping power of about 1.6×10^4 MeV g^{-1} cm^2). In Table I the results of this work as well as the inactivation data previously obtained by Brustad (9, 12) and Schambra and Hutchinson (17) are assembled. It appears that the molecular damage, measured either by the production of secondary radicals or by the inactivation of enzymes and phages, is largely influenced by the local distribution of the initial energy absorption. Thus, radiation with a low stopping power is from 2 to 5 times as efficient as the densely ionizing argon ions. The variation in yield found in this work seems to be much smaller than that reported by Müller et al. (5).

Dose-Effect Curves

In Fig. 5 the dose-effect curves for radical production in solid glycine by helium, carbon, and argon ions are presented. The curves are straight lines in this special plot up to a dose of about 10^7 rad, but it can be noticed that the slopes for all curves are less than 1.0. From this set of dose-effect curves two observations can be made:

1. The curves reach different saturation levels. The maximum number of radicals that can be trapped in solid glycine seems to decrease with increasing stopping power of the radiation.

2. The dose-effect curves passes through a maximum and goes down again for doses above 6 to 8×10^7 rad. This observation is similar to that previously reported by Rotblat and Simmons(19), who used 15-MeV

electrons and found that the radical concentration decreased for doses above 5×10^7 rad. They assert that they have proved that this decrease was due to thermal annealing from the high dose rate used. The radical decay in all solid substances, including glycine, increases at elevated temperatures, but in the experiments reported here the average sample temperature never reached such high values that thermal annealing alone can explain the large decrease in radical concentration (about a factor of 3). A more reasonable explanation is to assume that there is only a limited number of trapping sites, and that the radiation, in addition to producing radicals (that can be trapped at these sites), also destroys trapping sites. The different saturation levels in Fig. 5 can be explained by this latter process if it depends upon the stopping power.

Since the curves in Fig. 5 are not parallel it is evident that the results given in Table I depend upon the radiation dose as well as on the irradiation temperature. From Fig. 5 it can be found that Y_1/Y_2 for glycine varies from 2.3 for the dose 2×10^4 rad to about 4.8 for the highest doses used.

Qualitative changes in the glycine spectrum with large doses of electrons and α particles have previously been reported by Boag and Müller (20) and Müller et al. (5). In Fig. 6 are presented the spectral changes with increasing doses of helium, carbon, and argon ions. It appears that larger doses are necessary to give spectral changes when the stopping power increases. For argon ions very small changes are observed even with the largest doses used. The glycine spectrum observed after large doses of helium and carbon ions is very sensitive to microwave saturation. At low microwave power and with a small modulation amplitude six to eight poorly resolved hyperfine lines can be observed. The possibility suggested by Müller et al. (5) that

radicals already trapped absorb energy for a second time, resulting in a transformation or destruction of the radicals, might be an explanation. Thus, since no spectral changes or only very small ones were observed for argon ions when the stopping power is very large, it is reasonable to suppose that the radicals first must be trapped and that the transformation can take place when a new ion hits in the neighborhood. That is, high LET in the track is not enough to produce a transformation, it is also necessary to have a certain time lag between the two absorption events. This means that the transformation depends upon the density of the bombarding particles rather than upon the stopping power. In accordance with this the spectral changes were first observed for the helium ions.

A Model for the Formation of Radicals by Heavy Ions

The data presented in Figs. 2, 3, and 4 are all based on the radiation dose 1.5×10^{6} rad. If we assume that the bombarding particles were homogeneously distributed over the radiation field, it can be calculated that the distance between two tracks for this dose varies from 150 Å (helium ions) to about 1340 Å (argon ions). Consequently, the overlapping between two tracks is negligible and each track can be treated as independent of all others. From the above results the number of radicals per ion, N_s, or the density of radicals along the track can be calculated from

$$N_s = \frac{N}{D/eZA}$$

where N is the observed number of radicals per gram, D is the dose, given in coulombs, eZ is the charge of the bombarding particle, and A is the beam area. The parameter N_s can be correlated with the

apparent inactivation cross sections of biological test objects. The results of the work described here are presented in Fig. 7. All curves seem to be straight lines in this special plot.

It would be of interest to arrive at a model for the production of radicals by these densely ionizing particles. The goal would be to construct an expected curve, for the concentration of radicals in the track versus the stopping power, which can be compared with the experimental data in Fig. 7. In the following an attempt is made to construct such a model. The number of secondary radicals trapped along the track of a bombarding particle is assumed to be the sum of those produced by the energy deposited in the track core and those produced by the δ rays outside the core. When the stopping power of the bombarding particle increases the radical density increases and the saturation level is reached, with the result that the curve for yield versus stopping power starts to go down (as in Figs. 2, 3, and 4). The saturation level is first reached in the track core and then gradually also outside the core. Consequently, an increasing region around the center of the track is saturated with radicals, and only that portion of the δ-ray energy dissipated outside this region is available for additional radical production. It is reasonable to assume that, to a first approximation, the extra energy deposited in the saturated region is used to sustain a steady-state concentration of radicals. However because of an increase of the "temperature" in the track core, there is the possibility mentioned above that the radiation also destroys trapping sites, with the result that the radical density in the track core decreases with increasing stopping power. It would therefore be of considerable interest to obtain dose-effect curves for radiations with different stopping power for other compounds than glycine.

If, for example, the concentration of radicals in the track core varies with the radiation we would expect that different saturation levels would be reached, as for glycine.

Based on this qualitative model with a saturated region in the center of the track which increases with the stopping power, we can work out an expected curve for the radical concentration along the track. This calculation uses the δ-ray spectra presented by Brustad (9) and Dolphin and Hutchinson (8), as well as the experimental results for glycine in Figs. 3 and 5. According to Fig. 3 the radical concentration in the track increases linearly with the stopping power up to about 200 MeV g^{-1} cm^2 (the yield is constant). At this point the number of radicals in the track core has presumably reached its saturation value and the LET density (energy dissipated per volume) in the core represents the maximum that can be utilized for the production of secondary radicals. The next step is to calculate the total stopping power for which the δ-ray energy reaches this maximum LET density in the first layer outside the track core (the thickness of the layers should be infinitesimal, but in these calculations a thickness of 5 Å has been used), and then in the subsequent layers further out. This calculation necessitates knowledge about the following parameters:

(a) The maximum LET density that can be fully utilized to produce secondary radicals. From these experiments we assume that this value is equal to that attained in the track core of helium ions.

(b) The distribution of the δ-ray energy and its deposition outside the track core.

The maximum LET density can be calculated as follows. Approximately 54% of the total energy of the helium ion is dissipated in the track core where the initial ESR centers are produced. These radicals then

participate in secondary reactions and the secondary radicals formed are trapped in a region around the center of the track. This region is called the "radical track core." The volume of this core can be calculated by assuming that the concentration and distribution of radicals in the core of an individual helium ion is equal to the maximum overall concentration of radicals that can be trapped in the compound when large doses are used in which there is considerable overlapping between the tracks. This maximum concentration and distribution of radicals can easily be obtained for glycine from Fig. 5. (Since the results of this calculation are independent of the density of the compound, the value 1.0 has been used here for brevity.) For glycine the radicals produced by the energy dissipated in the track core seem to be spread out in a cylinder with radius 20 to 21 Å. If this value is used the volume of the radical track core and consequently the maximum LET density available for radical production can easily be calculated. It is further assumed that the δ-ray energy (46% of the total stopping power), to a first approximation, produces radicals outside this track core. The distribution of the δ-ray energy with the distance from the track core can be calculated from the δ-ray spectra presented either by Brustad(9) or by Dolphin and Hutchinson (8). These authors give the local energy dissipation as well as the LET of the δ-ray electrons. We can therefore roughly estimate the range of the δ-ray electrons and the percentage of the total energy deposited in the different layers outside the radical track core. The value of the stopping power for which one of these layers has reached its saturation level is calculated from

$$V \times LET_{max} = F\,(dE/dx),$$

where V is the volume of the layer, and F is the fraction of the total stopping power deposited in this layer. It is now possible to construct the curve for the number of radicals per ion versus the stopping power, since we assume that all extra energy deposited in the saturated region is unavailable for production of stable radicals. Since the δ-ray spectra calculated by Brustad and Dolphin and Hutchinson are different, we can construct two such curves; the results of calculations for glycine and alanine are shown in Fig. 8. The curves for alanine have been calculated by assuming that the maximum concentration of radicals that can be trapped in this compound is three times that found for glycine. The reason for this is the results obtained by Müller et al. (5). It appears that the experimental results fall between the two curves.

DISCUSSION

Two facts have been established by these experiments. Firstly, the types of secondary radicals produced in solid biochemicals seem to vary little with the type of radiation used. However, the results for glutathione indicate that the relative yields of the initial ESR centers may be influenced by the stopping power. Secondly, the curves for the radical yields versus the stopping power exhibit the same form as that previously reported for the inactivation of solid enzymes and for the loss of infectivity of T1 bacteriophage. The total variation in the radical yield within the LET range studied is, for the different substances, by a factor of from 2 to about 5. For the enzyme trypsin a surprisingly good correlation between the production of secondary radicals and the loss of enzyme activity was observed (Fig. 4).

From these data and from the inactivation data reported by Brustad (12) it can be calculated that when the samples have been at room temperature for approximately 20 minutes, 2.2 secondary radicals are trapped for each enzyme molecule inactivated. Decomposition of the spectra shows that there is approximately 0.7 sulfur radical per inactivated molecule. However, the number of sulfur radicals increases with time, and after one day at room temperature there are about 1.1 sulfur radicals per inactivated trypsin molecule. We should, however, bear in mind that these calculations are based on observations in which different samples have been used for the two types of measurements. Furthermore, the radiation doses in the inactivation experiments were much larger than used in these experiments. Similar direct correlations between the number of secondary radicals and the loss of enzyme activity have also been reported for ribonuclease by Hunt and Williams (21). However, correlations of this kind, in which one secondary radical is correlated with the inactivation of one macromolecule, are uncertain, and may lead to considerable error. The reason is that great problems still persist in the determination of the radical concentration. Furthermore, parameters such as the stability of the radicals, the vacuum in the sample, the bound water, etc., may also cause uncertainties.

A model for the production of radicals by heavy ions has been proposed. It is assumed that the radical concentration in the track is the sum of those produced in the radical track core and those produced by the δ rays outside this core. The results indicate that the concentration of radicals in the core reaches the saturation level for helium ions with a stopping power of 190 MeV $g^{-1}cm^2$. With increasing stopping power the saturation level will be reached in regions farther and farther out

from the center of the track, and the cross section of the saturated area will increase with the stopping power. From the dose-effect curves for glycine in Fig. 5 it can be calculated that the track area increases with Z^2 (Z is the atomic number of the bombarding particle). Norman and Spiegler (22) have proposed a similar relationship between the cross section of the decomposed area and the LET for fission fragments.

The model here proposed for the production of secondary radicals embodies some of the ideas suggested by Dolphin and Hutchinson (8). These authors use the density and distribution of the primary ionizations along the track of the ionizing particle as the basis for the biological end effect, and pay little attention to the secondary reactions between these two steps. In our work we have studied the formation of the secondary radicals, and Fig. 4 shows that there is a good correlation between these radicals and the biological end effect. There are still large gaps in our knowledge about what is occurring between the primary energy absorption and the trapping of the secondary radicals, as well as between this step and the inactivation, which can be measured only after the solid samples have been dissolved in water. We know from Brustad's experiments on trypsin (12) that temperature influences some of the secondary reactions between the initial absorption event and the end effect as measured by the loss of enzymatic activity, and some recent ESR experiments show that the temperature similarly influences the reactions leading to the formation of the secondary radicals (16).

ACKNOWLEDGMENTS

I wish to express my gratitude to Professor C. A. Tobias and his group for the hospitality and working facilities offered me at Donner Laboratory.

It is a pleasure to acknowledge financial support from the U. S. Atomic Energy Commission and the National Aeronautics and Space Administration.

REFERENCES

1. F. Patten and W. Gordy, Temperature effects on the formation of free radicals in the amino acids. Radiation Research 14, 573 – 589 (1961).
2. F. Patten and W. Gordy, Temperature effects on the free radical formation and electron migration in irradiated proteins. Proc. Natl. Acad. Sci. U. S. 46, 1137 - 1144 (1961).
3. T. Henriksen, Radiation-induced free radicals in sulfur compounds. ESR studies in the polycrystalline state. J. Chem. Phys. 37, 2189 - 2195 (1962).
4. T. Henriksen, T. Sanner, and A. Pihl, Secondary processes in proteins irradiated in the dry state. Radiation Research 18, 147 –162 (1963).
5. A. Müller, P. E. Schambra, and E. Pietsch, Comparative ESR measurements of the radical production in amino acids by Po^{210} - alpha and Co^{60} – gamma radiation. Int. J. Rad. Biol. 7, 587 – 599 (1963).
6. K. Stratton and A. Koehler, Free radical formation in proton irradiated enzymes. Radiation Research 22, 240 (1964) (Abstract).
7. R. E. Zirkle and C. A. Tobias, Effects of ploidy and LET on radiobiological survival curves. Arch. Biochem. Biophys. 47, 282 – 306 (1953).
8. G. W. Dolphin and F. Hutchinson, The action of fast carbon and heavier ions on biological materials. Radiation Research 13, 403 –414 (1960).
9. T. Brustad, Heavy ions and some aspects of their use in molecular and cellular radiobiology. Advan. Biol. Med. Phys. 8, 161 – 224 (1962).

10. C. A. Tobias and T. R. Manney, Some molecular and cellular effects of heavily ionizing radiation. Ann. N. Y. Acad.Sci. 114, 16 - 24 (1964).

11. C. A. Tobias and P. W. Todd, Analysis of the effects of high LET radiations on various strains of cells. In The Biological Effects of Neutron Irradiation, Intern. Atomic Energy Agency, Vienna, 1964.

12. T. Brustad, Heat as a modifying factor in enzyme inactivation by ionizing radiation. In The Biological Effects of Neutron Irradiations, Intern. Atomic Energy Agency, Vienna, 1964.

13. T. Brustad, P. Ariotti, and J. Lyman, Experimental setup and dosimetry for investigating biological effects of densely ionizing radiation. Lawrence Radiation Laboratory Report UCRL-9454, Oct. 1960 (unpublished).

14. W. H. Barkas and M. J. Berger, Tables of energy losses and ranges of heavy charged particles. NASA report SP -3010, 1964.

15. T. Henriksen, ESR studies on the formation of sulfur radicals in irradiated cysteine, glutathione, and djenkolic acid. J. Chem. Phys. 36, 1258 - 1262 (1962).

16. T. Henriksen, Effect of the irradiation temperature on the production of free radicals in solid biological compounds exposed to various ionizing radiation (submitted to Radiation Research).

17. P. E. Schambra and F. Hutchinson, The action of fast heavy ions on biological material. Radiation Research 24, 514 - 526 (1964).

18. T. Henriksen, On the mechanisms for radiation damage and repair in solid biological systems as revealed by ESR spectroscopy. In

Solid State Physics in Medicine and Biology, (S. J. Wyard, Editor) McGraw Hill Book Co., New York (in press).

19. J. Rotblat and J. A. Simmons, Dose-response relationship in the yield of radiation-induced free radicals in amino acids. Phys. Med. Biol. 7, 489 - 498 (1963).

20. J. W. Boag and A. Müller, Changes in the electron spin resonance spectrum of glycine with increasing doses of radiation. Nature 183, 831 (1958).

21. J. W. Hunt and J. F. Williams, Radiation damage in dry ribonuclease. Yields of free radicals and other chemical lesions compared with inactivation efficiency. Radiation Research 23, 26 - 52 (1964).

22. A. Norman and P. Spiegler, A thermal decomposition model for radiation damage in solids. Radiation Research 16, 599 (1962) (Abstract).

Table I. Effect of the stopping power on the radiation yield.[a]

Compound	Irradiation temperature	Parameter measured	Y_1/Y_2	Reference
DNase	Room temp	Inactivation	2.3	9,12
Lysozyme	Room temp	Inactivation	2.1	9,12
Trypsin[b]	Room temp	Inactivation	2.3	9,12
Trypsin[b]	Room temp	Inactivation	1.8	9,12
T1 Bacteriophage	Room temp	Inactivation	3.0	17
ϕX-174 Bacteriophage	Room temp	Inactivation	3.4	17
Trypsin[c]	Room temp	Radicals	2.4	This work
Trypsin[c]	Room temp	Radicals	3.1	This work
Glycine	300° K	Radicals	4.1	This work
Glycine	200° K	Radicals	3.7	This work
Glycine	100° K	Radicals	3.2	This work
Alanine	Room temp	Radicals	3.3	This work
Glutathione	Room temp	Radicals	3.0	This work
Cytidine	Room temp	Radicals	2.3	This work
Cytosine	Room temp	Radicals	5.1	This work
Guanosine	Room temp	Radicals	3.6	This work

a. The radical yields refer to samples that have been at room temperature approximately 20 minutes before the measurements. Y_1 is the yield observed for radiation with a low stopping power (the flat portion of the curves in Figs. 2, 3, and 4), and Y_2 refers to the results obtained for argon ions with a stopping power of approximately 1.6×10^4 MeV g^{-1} cm^2.

b. These data refer to two separate experiments on trypsin. The reason for the differences may be that two different trypsin samples were used.

c. In order to test the possibility mentioned under b ESR experiments were carried out with two different types of trypsin. The largest value (3.1) was obtained with noncrystalline powder, whereas the other results are taken from experiments on crystalline trypsin. It is therefore reasonable to suppose that the physical state of the solid compound also can explain the differences observed by Brustad.

FIGURE LEGENDS

Fig. 1. The qualitative spectra of reduced glutathione irradiated with different types of heavy ions. Both the irradiations and the measurements have been carried out at room temperature. The spectra were recorded after the samples had been kept at this temperature for about 20 minutes. Dose 1.5×10^6 rad.

Fig. 2. The yield of secondary radicals as a function of the stopping power for several compounds. The data are based on the spectra recorded after the samples have been at room temperature for approximately 20 minutes. The results for the aromatic compounds cytosine and cytidine have been multiplied by a factor 10 in order to be plotted on the same scale as the others. The ordinate corresponds to the G value (number of radicals per 100 eV absorbed). However, relative values are more reliable than the absolute determinations.

Fig. 3. The yield of secondary radicals as a function of the stopping power for glycine. Conditions as in Fig. 2. The different curves indicate different irradiation temperatures.

Fig. 4. The radiation effect in solid trypsin, as measured by the loss of enzyme activity [these data are taken from Brustad (12)] and by the production of secondary radicals as a function of the stopping power. The conditions for the radical measurements are the same as in Fig. 2. The inactivation curve for solid trypsin is exponential with respect to the radiation dose. The parameter used for the inactivation is the reciprocal of the D_{37} dose. In this figure the original data have been recalculated and are given in relative units in order to be plotted on the same figure. The flat portion of the curve was given the value 2.5.

Fig. 5. Production of secondary radicals in solid glycine as a function of the radiation dose of helium, carbon and argon ions.

Fig. 6. Qualitative changes in the polycrystalline glycine spectrum with increasing doses of helium, carbon, and argon ions.

Fig. 7. The density of radicals along the track of a bombarding particle as a function of the stopping power. The data were calculated by assuming that the ionizing particle penetrates 1 gram spread out over an area of 1 cm^2 with uniform stopping power along the track.

Fig. 8. The calculated number of secondary radicals along the track of the bombarding particle versus the stopping power for glycine and alanine (see text). The expected curves can be given by $N_s = (1-k)\, dE/dx$, where the variable parameter k, for each value of the stopping power, gives the fraction of the deposited energy that is unavailable for radical production. For small LET values k is zero (the straight dashed lines), and it increases with the stopping power, since the saturated region around the track gradually becomes larger. The curve D + H is based on the δ-ray spectrum of Dolphin and Hutchinson (8) and the curve B on the spectrum given by Brustad (9). The data observed for the different ions used in these experiments are also included.

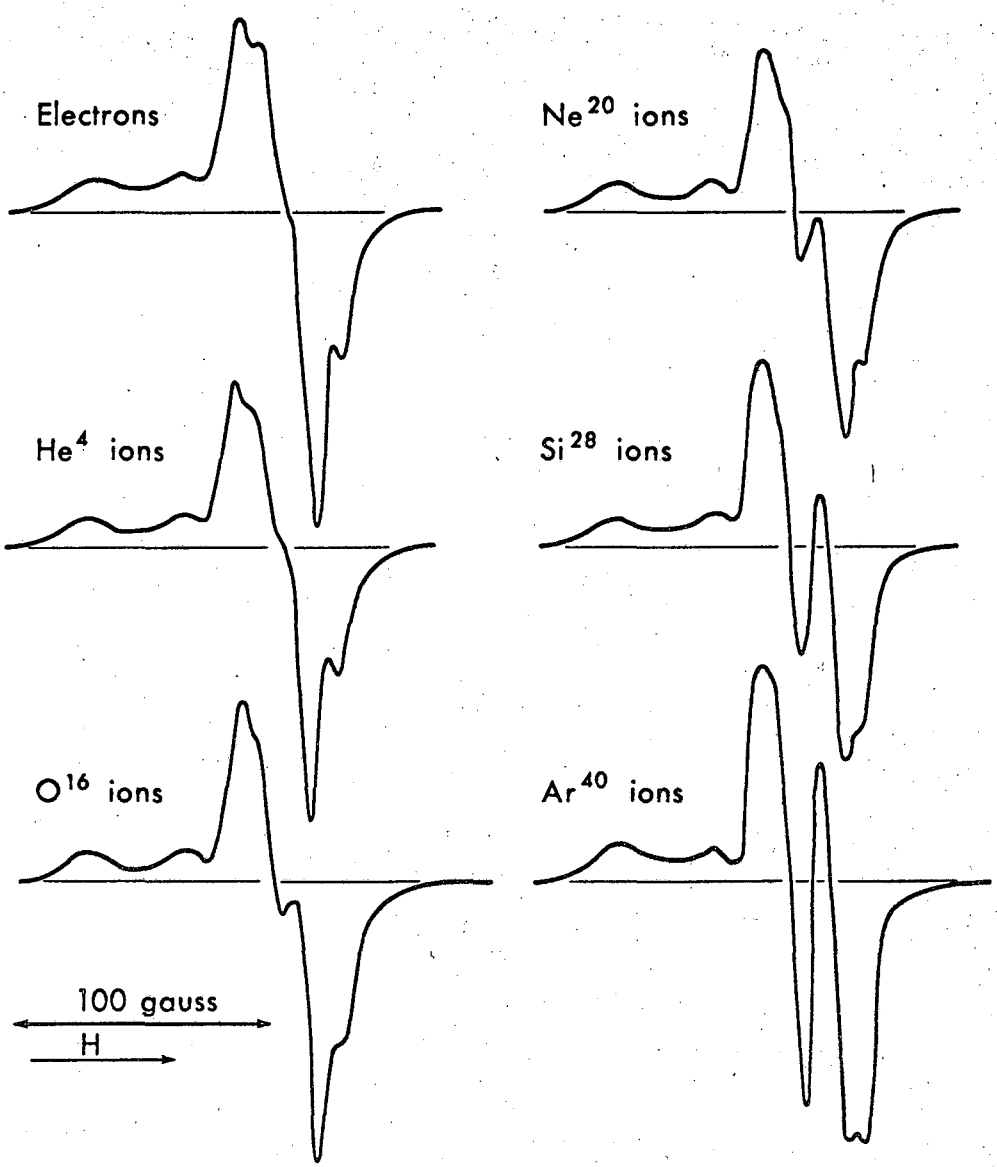

Fig. 1

MUB-5013

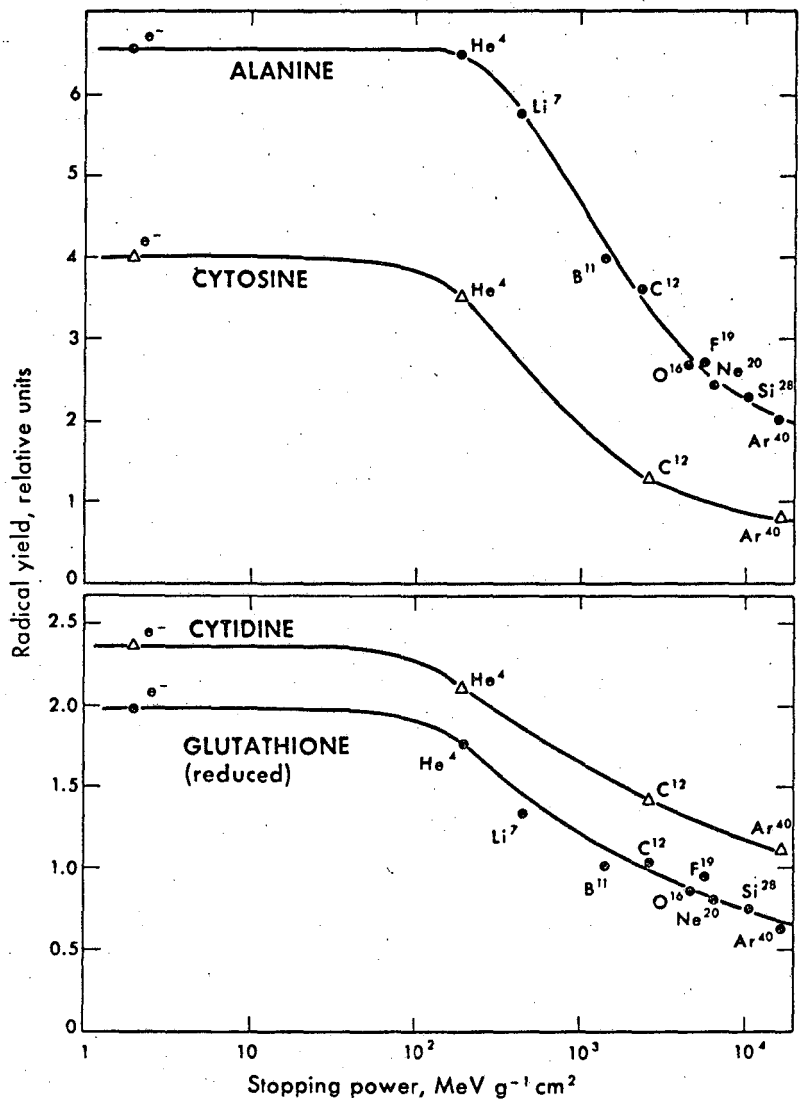
ALANINE
CYTOSINE
CYTIDINE
GLUTATHIONE
(reduced)
e⁻
He⁴
Li⁷
B¹¹
C¹²
O¹⁶
F¹⁹
Ne²⁰
Si²⁸
Ar⁴⁰
Radical yield, relative units
Stopping power, MeV g⁻¹ cm²
MUB-5012

Fig. 2

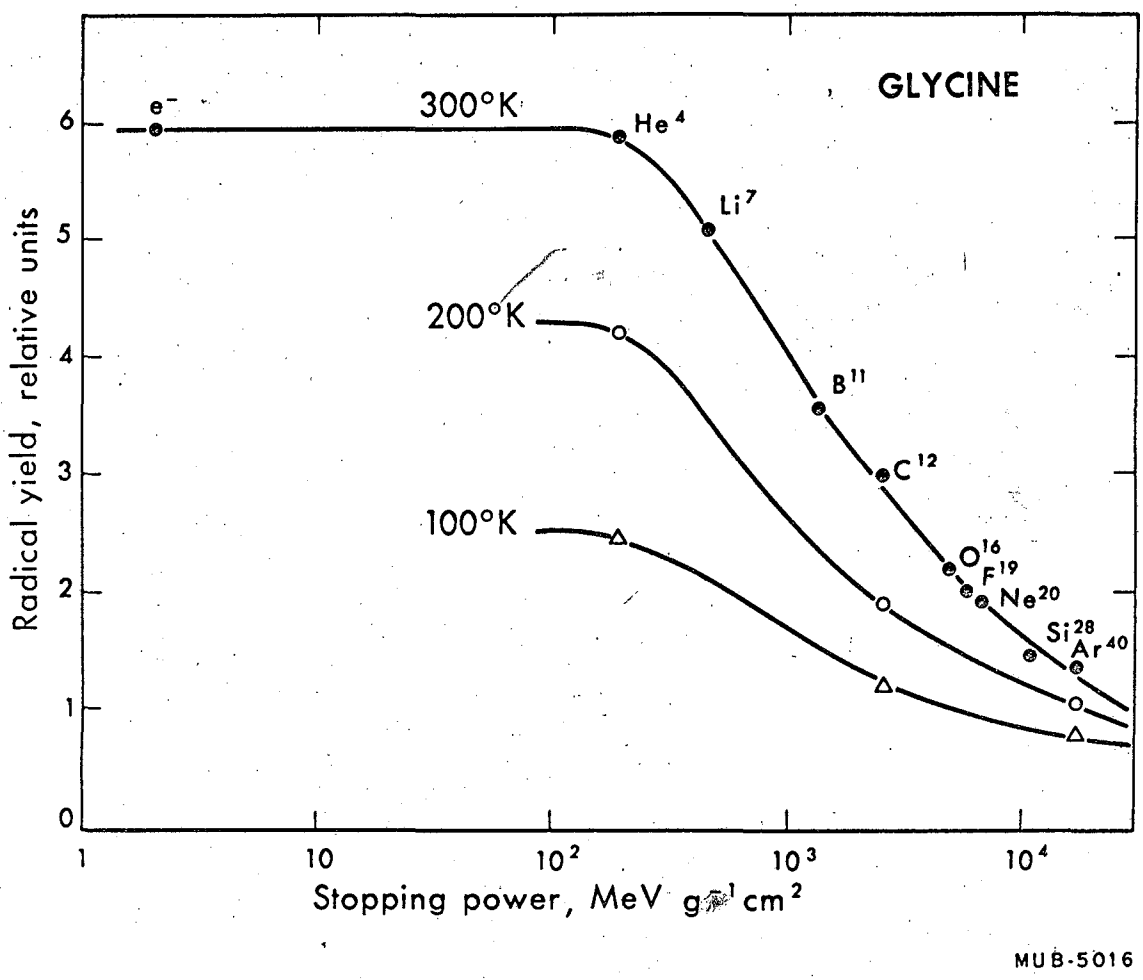
GLYCINE
300°K
200°K
100°K
e⁻
He⁴
Li⁷
B¹¹
C¹²
O¹⁶
F¹⁹
Ne²⁰
Si²⁸
Ar⁴⁰
Radical yield, relative units
Stopping power, MeV g⁻¹ cm²
0
1
2
3
4
5
6
1
10
10²
10³
10⁴
MUB-5016

Fig. 3

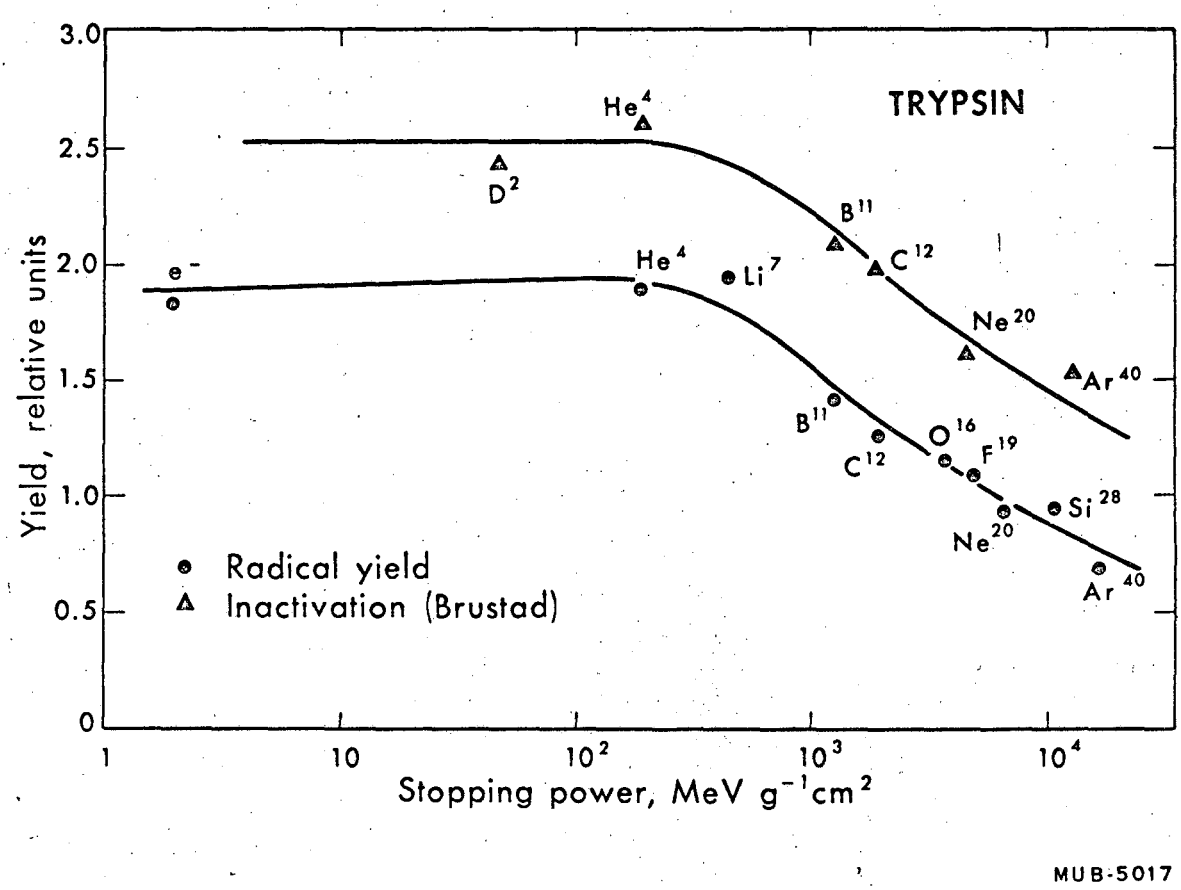
TRYPSIN
Yield, relative units
Stopping power, MeV g⁻¹cm²
Radical yield
Inactivation (Brustad)
e⁻
He⁴
D²
Li⁷
B¹¹
C¹²
Ne²⁰
Ar⁴⁰
O¹⁶
F¹⁹
Si²⁸
MUB-5017

Fig. 4

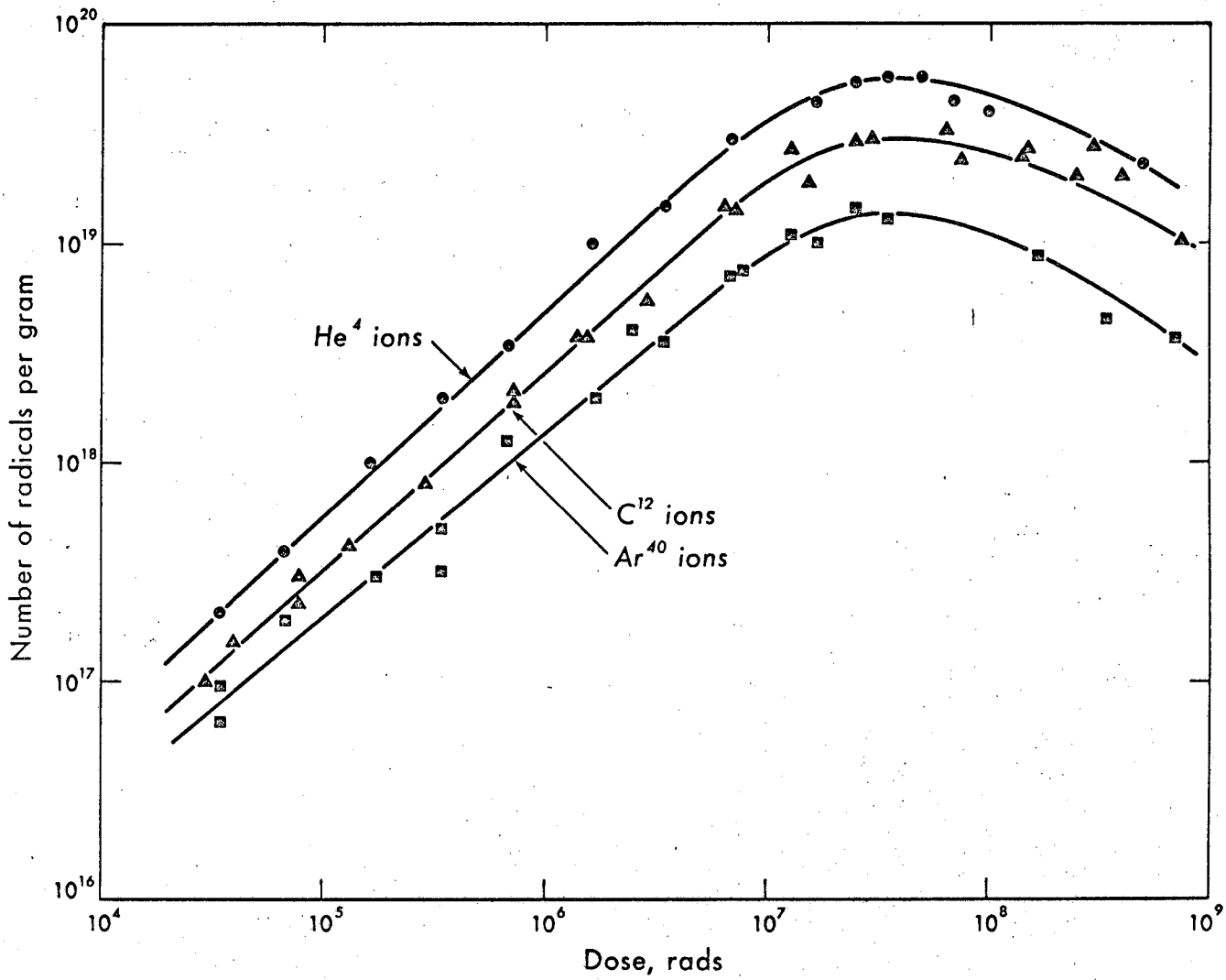
Number of radicals per gram
10^{20}
10^{19}
10^{18}
10^{17}
10^{16}
10^4
10^5
10^6
10^7
10^8
10^9
Dose, rads
He^4 ions
C^{12} ions
Ar^{40} ions
MUB-5011

Fig. 5

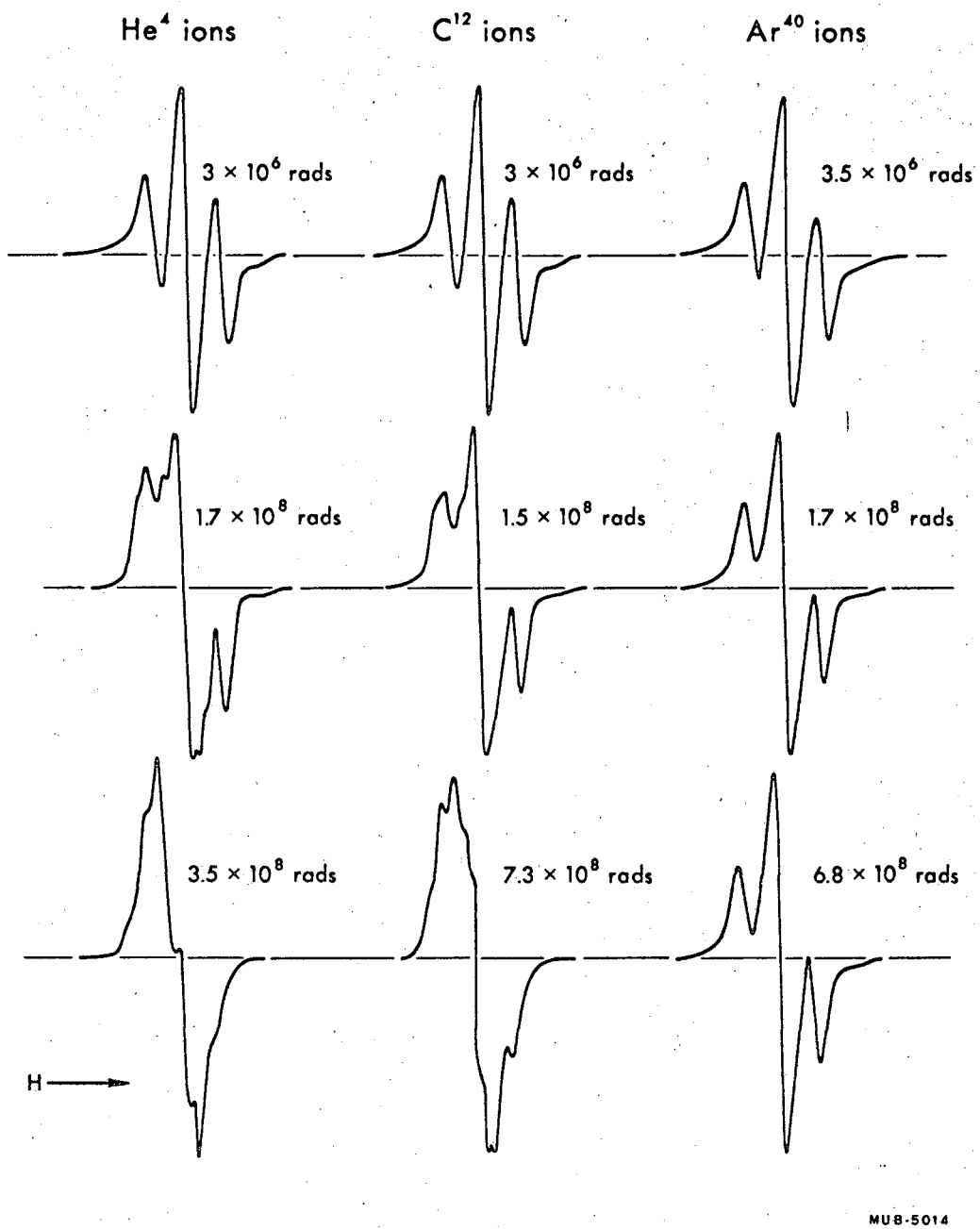
He⁴ ions
C¹² ions
Ar⁴⁰ ions
3 × 10⁶ rads
3 × 10⁶ rads
3.5 × 10⁶ rads
1.7 × 10⁸ rads
1.5 × 10⁸ rads
1.7 × 10⁸ rads
3.5 × 10⁸ rads
7.3 × 10⁸ rads
6.8 × 10⁸ rads
H
MUB-5014

Fig. 6

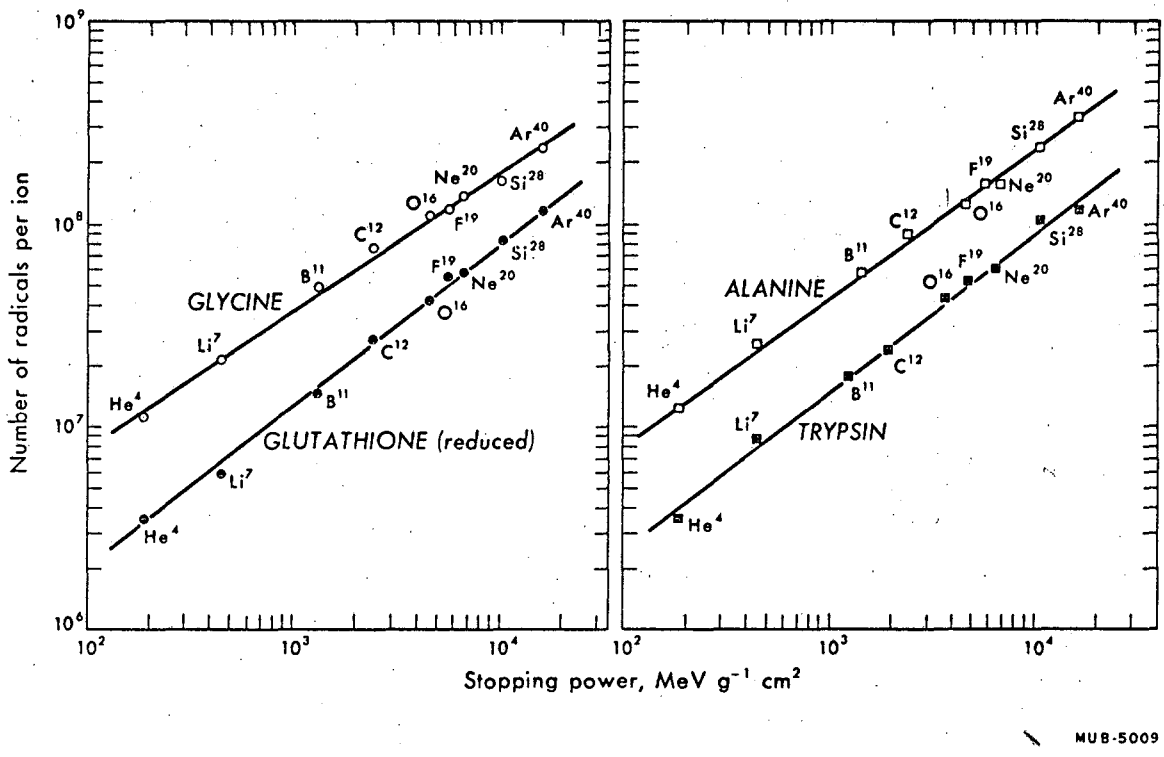
Number of radicals per ion
Stopping power, MeV g⁻¹ cm²
GLYCINE
GLUTATHIONE (reduced)
ALANINE
TRYPSIN
He⁴
Li⁷
B¹¹
C¹²
O¹⁶
F¹⁹
Ne²⁰
Si²⁸
Ar⁴⁰
MUB-5009

Fig. 7

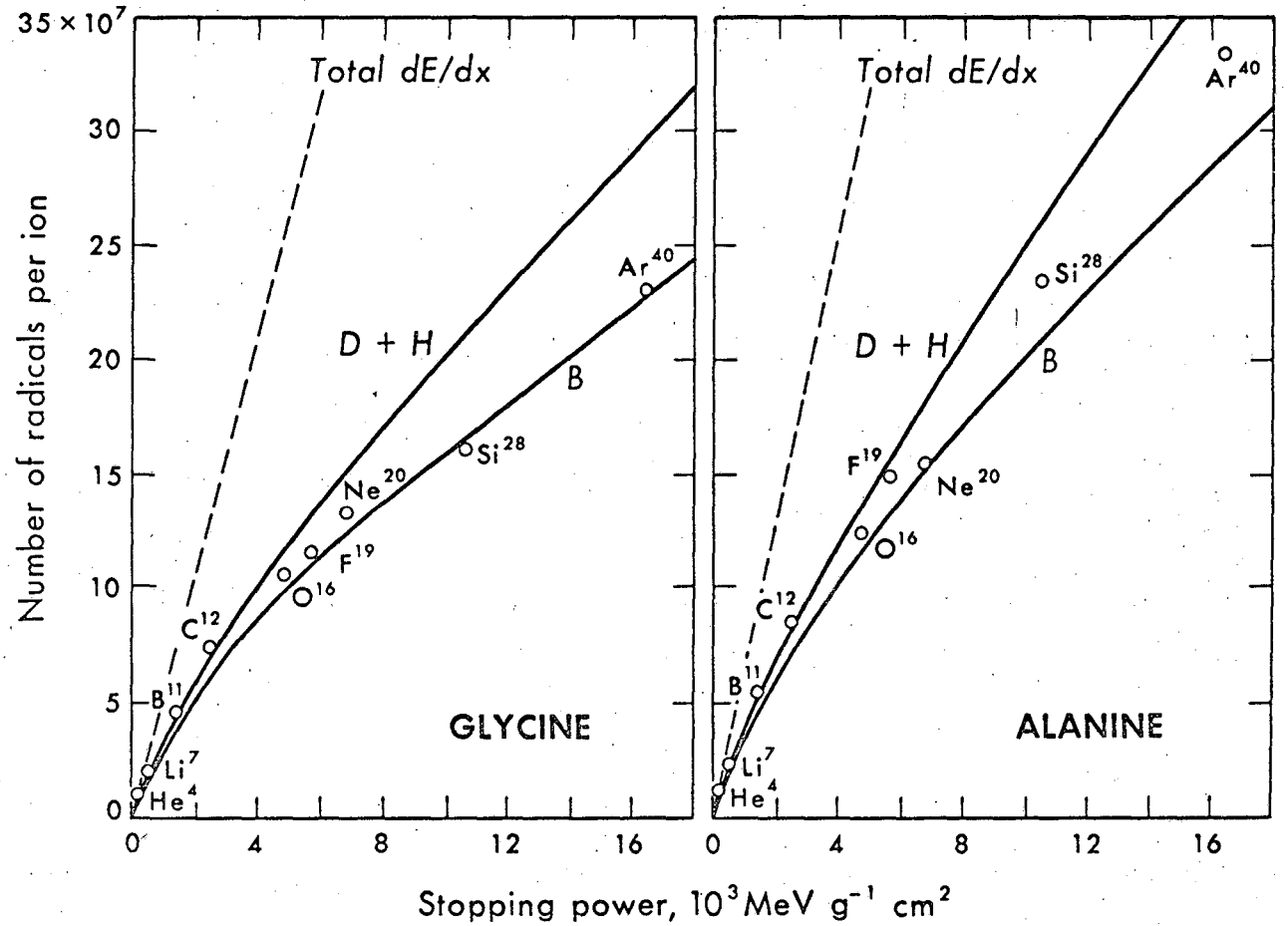
35 × 10^7
Number of radicals per ion
Total dE/dx
D + H
B
Ar^40
Si^28
Ne^20
F^19
O^16
C^12
B^11
Li^7
He^4
GLYCINE
ALANINE
0
4
8
12
16
Stopping power, 10^3 MeV g^-1 cm^2
MUB-5008

Fig. 8